Asociación Argentina
de Mecánica Computacional

Mecánica Computacional Vol XXXIII, págs. 1179-1192 (artículo completo)
Graciela Bertolino, Mariano Cantero, Mario Storti y Federico Teruel (Eds.)
San Carlos de Bariloche, 23-26 Setiembre 2014

AN IMPLEMENTATION OF THE GENERALIZED MAXWELL VISCOELASTIC CONSTITUTIVE MODEL

Claudio A. Careglio[b], Cristian Canales[a], Luc Papeleux[a], Jean-Philippe Ponthot[a], Carlos G. García Garino[b] and Anibal E. Mirasso[b]

[a]*Department of Aerospace & Mechanical Engineering, Université de Liège, Belgium, ccanales@ulg.ac.be, L.Papeleux@ulg.ac.be, JP.Ponthot@ulg.ac.be*

[b]*Facultad de Ingeniería and ITIC, , Universitario Universidad Nacional de Cuyo. Centro Universitario, 5500 Mendoza, Argentina, ccareglio@uncu.edu.ar, cgarcia@itu.uncu.edu.ar, aemirasso@uncu.edu.ar*

Keywords: Viscoelasticity, generalized Maxwell, numerical model, sensitivity to constitutive parameters.

Abstract. Viscoelastic problems deserve great interest in Computational Mechanics literature. In the last years different approaches have been proposed in order to model viscoelastic problems, as in the case of the generalized Maxwell model and its numerical implementation.
In particular Kaliske and Rothert (M. Kaliske and H. Rothert, Comput. Mech., 19(3): 228-239 (1997)) discussed basic reological models and the formulation of a generalized Maxwell model and the corresponding implementation of three dimensional viscoelastic model both for small and large strain cases.
The numerical implementation addressed by Kaliske and Rothert is quite simple for small strain case and can be extended to a large strain format amenable to be included in finite element codes SOGDE and Metafor.
The implementation of the discussed model in a 1D constitutive model, written in Matlab, is addressed. The well known relaxation and creep tests are simulated and compared with analytical results. Furthermore, the influence of constitutive parameters on the viscoelastic response is discussed. In addition, the model is implemented in Finite Element codes and the obtained results are compared with the 1D ones.

1 INTRODUCTION

Materials with both elastic and viscous behaviors are usually called "viscoelastics". An essential feature of them is the time-dependent response. These materials have received great scientific and technological interest due to the diversity of its applications and consequently different approaches have been proposed to model viscoelastic response, see Fancello et. al (2006,2008) and Bonet (2001) for instance. Some common applications of these materials are human cervical spine (Shim et. al, 2005), bovine cortical bone (Bekker et. al, 2014), vibration absorbers (Saidi, 2011), tires (Lee, 2011), among others.

There several differential constitutive models (Ottosen, 2005; Drozdov, 1996) able to represent the response of viscoelastic materials. One such model is the Kelvin-Voigt, currently implemented in Metafor code (Ponthot, 1995, 2002). A more general is the so called generalized Maxwell or Wiechert model. A feature of the latter is to consider that the relaxation occurs at a distribution of times.

Applications related to biomechanics, for instance, make it necessary to implement this constitutive model numerically in large strain finite element codes such as SOGDE (García Garino, 1993; Careglio et. al, 2005; García Garino et. al, 2006) and Metafor.

In this work we performed the numerical implementation addressed by Kaliske and Rothert (1997) of the generalized Maxwell model. In particular, this model is implemented in a one-dimensional code as well as a finite element one.

Several numerical experiments are performed. In particular, relaxation and creep problems are studied and the results are compared with analytical ones. Then, the case of constant strain rate is studied with the different numerical implementations that have been made in this work.

In addition, sensitivity to constitutive parameters of the generalized Maxwell model and numerical implementation from Kaliske and Rothert (1997) are presented.

A summary of the viscoelastic and numerical models are briefly presented in section 2 of this paper. The results of numerical simulations are shown in section 3. Finally, in section 4 the conclusions of the work are provided.

2 VISCOELASTIC AND NUMERICAL MODELS

In this section, the viscoelastic model used and the numerical model is briefly described, and can be found in greater detail in the work of Kaliske and Rothert (1997).

The viscoelastic model corresponds to a generalized Maxwell one, as shown in Figure 1, where μ_0 is the elastic material constant of the so called Hooke-element and μ_j are the elastic material constant of the Maxwell-element with j=1..N. For these elements the coefficient of viscosity is η_j. This coefficient can be expressed in terms of the relaxation time τ_j as $\eta_j = \tau_j \mu_j$.

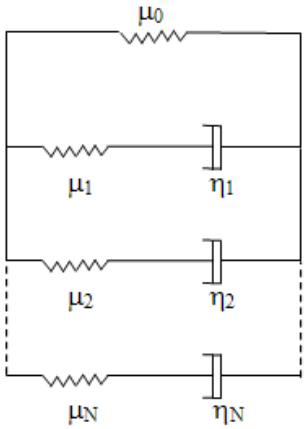

Figure 1: Generalized Maxwell model.

In the numerical model for linear viscoelasticity and one-dimensional case the current state of stress is computed by:

$$\sigma^{n+1} = \mu_0 \, \varepsilon^{n+1} + \sum_{j=1}^{N} h_j^{n+1} \tag{1}$$

where ε^{n+1} is the current strain and h^{jn+1} are the internal stress variables given by:

$$h_j^{n+1} = \exp\left(-\frac{\Delta t}{\tau_j}\right) h_j^n + \gamma_j \frac{1-\exp\left(-\frac{\Delta t}{\tau_j}\right)}{\frac{\Delta t}{\tau_j}} \left[\sigma_0^{n+1} - \sigma_0^n\right] \tag{2}$$

Equations (1-2) have been implemented in a one dimensional code for one Gauss point.

The extension to the three-dimensional case is:

$$\underline{\sigma}^{n+1} = \underline{\sigma}_0^{n+1} + \sum_{j=1}^{N} \underline{h}_j^{n+1} \tag{3}$$

with:

$$\underline{\sigma}_0^{n+1} = \underline{\underline{C}}^e \, \underline{\varepsilon}^{n+1} \tag{4}$$

$$\underline{h}_j^{n+1} = \exp\left(-\frac{\Delta t}{\tau_j}\right) \underline{h}_j^n + \gamma_j \frac{1-\exp\left(-\frac{\Delta t}{\tau_j}\right)}{\frac{\Delta t}{\tau_j}} \left[\underline{\sigma}_0^{n+1} - \underline{\sigma}_0^n\right] \tag{5}$$

where $\underline{\underline{C}}^e$ is the constitutive elastic tensor and $\gamma_j = \mu_j/\mu_0$ is the normalized elastic material constant. The constitutive viscoelastic tensor $\underline{\underline{C}}^{v,n+1}$ is given by:

$$\underline{\underline{C}}^{v,n+1} := \frac{\partial \underline{\sigma}^{n+1}}{\partial \underline{\varepsilon}^{n+1}} = \left\{ 1 + \sum_{j=1}^{N} \gamma_j \frac{1 - \exp\left(-\frac{\Delta t}{\tau_j} \right)}{\frac{\Delta t}{\tau_j}} \right\} \underline{\underline{C}}^{e,n+1} \tag{6}$$

Equations (3-6) have been implemented in a finite element code.

Alternatively, the three-dimensional case, in order to be initially considered for large strains, it can be conveniently expressed as:

$$\underline{\sigma}^{n+1} = \kappa l_{\underline{\varepsilon}}^{n+1} \underline{\mathbf{1}} + dev\underline{\sigma}_0^{n+1} + \sum_{j=1}^{N} \underline{h}_j^{n+1} \tag{7}$$

$$\underline{h}_j^{n+1} = \exp\left(-\frac{\Delta t}{\tau_j} \right) \underline{h}_j^{n} + \gamma_j \frac{1 - \exp\left(-\frac{\Delta t}{\tau_j} \right)}{\frac{\Delta t}{\tau_j}} \left[dev\underline{\sigma}_0^{n+1} - dev\underline{\sigma}_0^{n} \right] \tag{8}$$

$$\underline{\underline{C}}^{v,n+1} = \kappa \left(\underline{\mathbf{1}} \otimes \underline{\mathbf{1}} \right) + \left\{ 1 + \sum_{j=1}^{N} \gamma_j \frac{1 - \exp\left(-\frac{\Delta t}{\tau_j} \right)}{\frac{\Delta t}{\tau_j}} \right\} \times 2\mu_0 \left[\underline{\underline{\mathbf{I}}} - \frac{1}{3} \left(\underline{\mathbf{1}} \otimes \underline{\mathbf{1}} \right) \right] \tag{9}$$

where κ is the bulk modulus and *dev* denote the deviatoric part of the tensors. Finally, the equations (7) to (9) have been preliminarily implemented in Metafor.

3 NUMERICAL SIMULATIONS

In this section several problems are considered in order to evaluate the response of the numerical model described above and the different implementations.

3.1 Benchmarks

Several benchmarks are performed in this section. The results are compared with analytical ones. Both relaxation and creep tests are considered, which are usually used to assess the time-dependent behavior of viscoelastic materials.

3.1.1 Relaxation test with one branch of Maxwell

The first benchmark is the simulation of the relaxation test. The model consists of one Hooke-element and one Maxwell-element. The model is shown in Figure 2. The strain is applied instantaneously and remained constant over time.

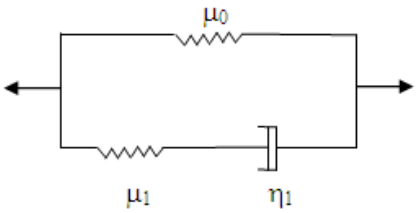

Figure 2: Generalized Maxwell model with one branch.

For this case the analytic solution it can be expressed as:

$$\sigma(t)=\left(\mu_0+\mu_1 e^{\frac{-t}{\tau_1}}\right)\varepsilon \tag{10}$$

The material properties are shown in Table 1. The applied strain is ε=2 while the interval time is 0s< t≤1s with Δt=0.1s.

μ_0=10 N/mm^2
μ_1=10 N/mm^2
η_1=10 MPa s
τ_1=1s

Table 1: Material properties.

The stress history is shown in Figure 3. For numerical results the equations (1-2) are used, while for the analytical ones the equation (10) is employed.. It can be seen that for relaxation test numerical results are able to reproduce the behavior of the analytical ones with a good agreement.

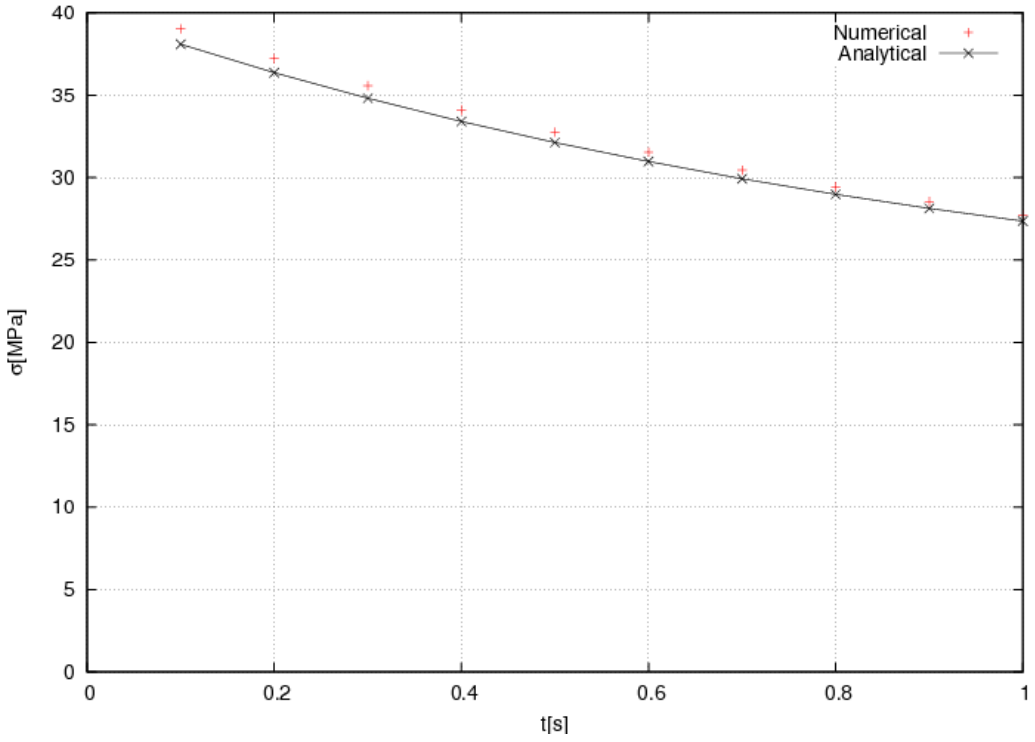

Figure 3: Stress history for relaxation test.

3.1.2 Relaxation test with one branch of Maxwell and different relaxation times

The second benchmarks correspond to the relaxation test and the same configuration model of the Figure 2. In this case four different relaxation times are considered. The properties of the material are shown in Table 2. In this case the simulations are carried out with ε=0.01, in the interval 0s< t≤20s for Δt=0.01s. For this case the relaxation times are τ_1=1,5,10,20 seconds.

μ_0=4 N/mm^2
μ_1=10 N/mm^2
η_1=10 MPa s (τ_1=1s)
η_1=50 MPa s (τ_1=5s)
η_1=100 MPa s (τ_1=10s)
η_1=200 MPa s (τ_1=20s)

Table 2: Material properties.

The analytical results are computed from equation (10) and compared with the numerical ones. The evolution of the stress in time is plotted in Figure 4. In all cases, the agreement of the obtained results is excellent.

It can be seen from the curve corresponding to τ_1=1s that the numerical model is able to reproduce the characteristic asymptotic behavior of the stress for some cases of the relaxation test.

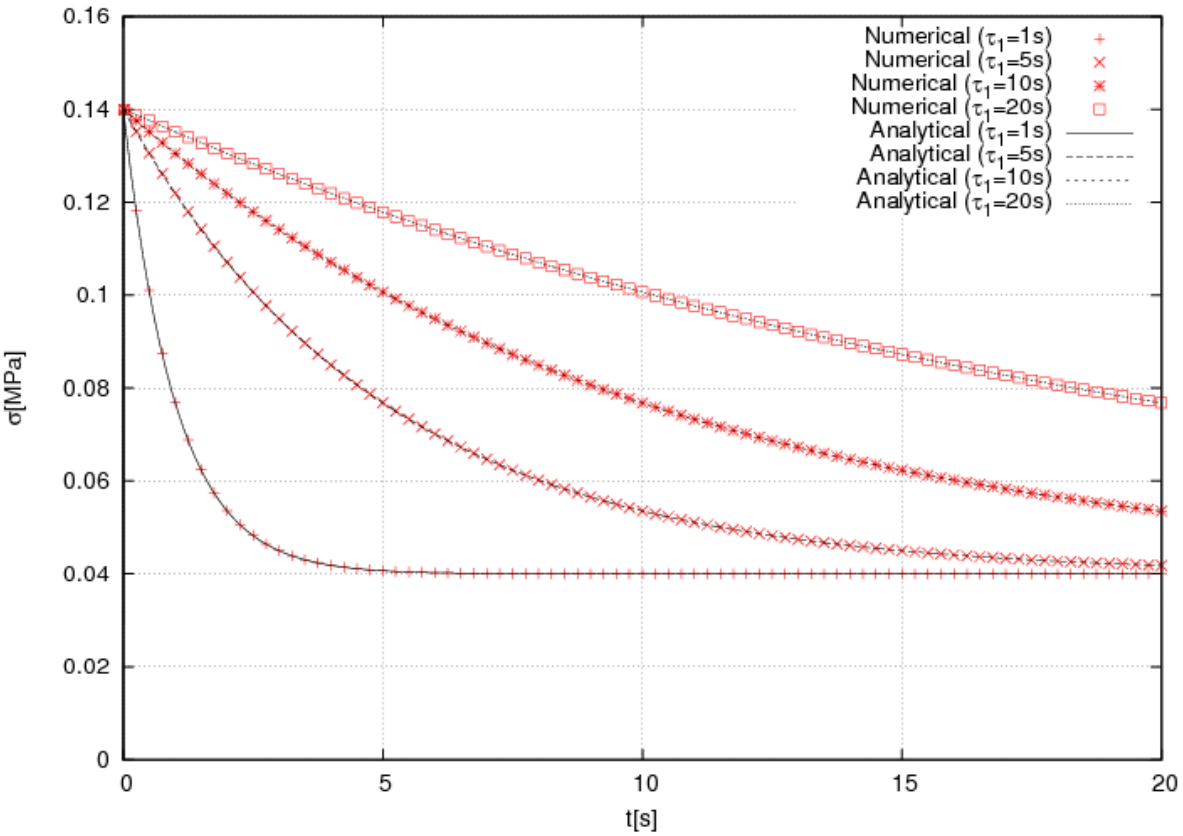

Figure 4: Stress history for relaxation test.

From a point of view of the sensitivity to constitutive parameters it can be said that when relaxation time τ_1 decreases due to viscosity η_1 decreases, the stress is lower for the same time. Further, according as τ_1 decreases the stress behavior tends to be asymptotic.

The influence of relaxation time τ_1 on stress for the maximum time reached (t_{max}=20s) is plotted in Figure 5. Consistent with results of Figure 4 when τ_1 increases greater values of stress are obtained.

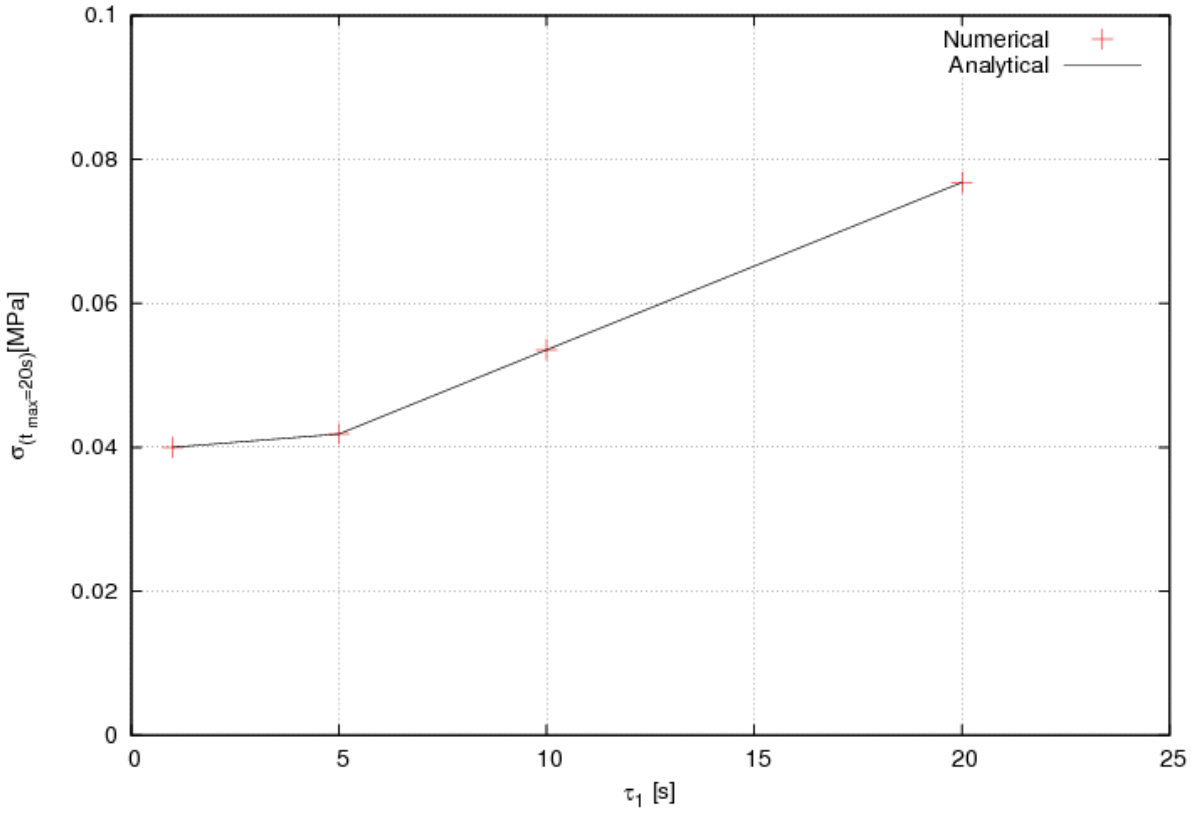

Figure 5: Sensitivity to relaxation time of the generalized Maxwell model with one branch.

3.1.3 Creep test with one branch of Maxwell

The third benchmark is the simulation of the creep problem for one Hooke-element and one Maxwell-element. The stress is applied instantaneously and remained constant over time. For this case, the analytical solution is given by:

$$\varepsilon(t) = \frac{\sigma_0}{\mu_0}\left(1 - \frac{\mu_1}{\mu_0+\mu_1} e^{\frac{-t}{\tau_1}\left(\frac{\mu_1}{\mu_0+\mu_1}\right)}\right) \tag{11}$$

The material properties are the same as those of Table 1. The applied stress is σ_0=100N/mm^2 in the time 0s< t≤10s with Δt=0.1s.

It should be clarified that the implemented code is strain-driven type. Taking this into account, from equation (11) and previous data is possible to obtain the strain history that is shown in Figure 6.

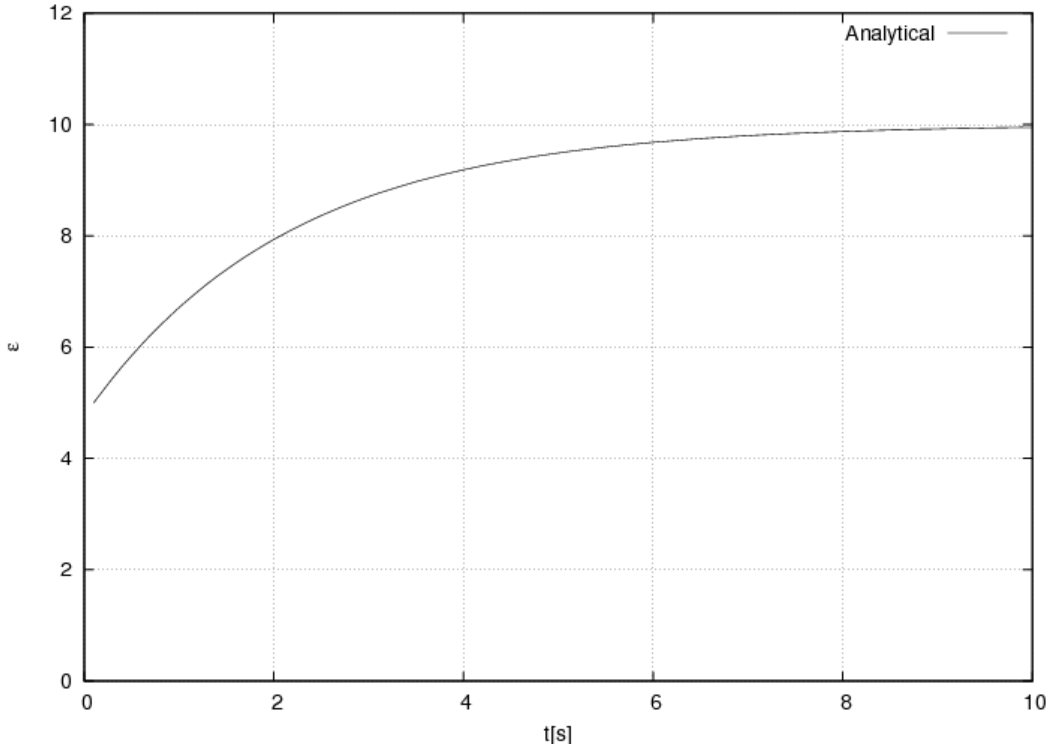

Figure 6: Strain history for creep test.

It can be seen in Figure 7 that the numerical results obtained from the strain-history recovery the corresponding stress-history. Also, it can be observed that a good agreement between numerical and analytical values is reached.

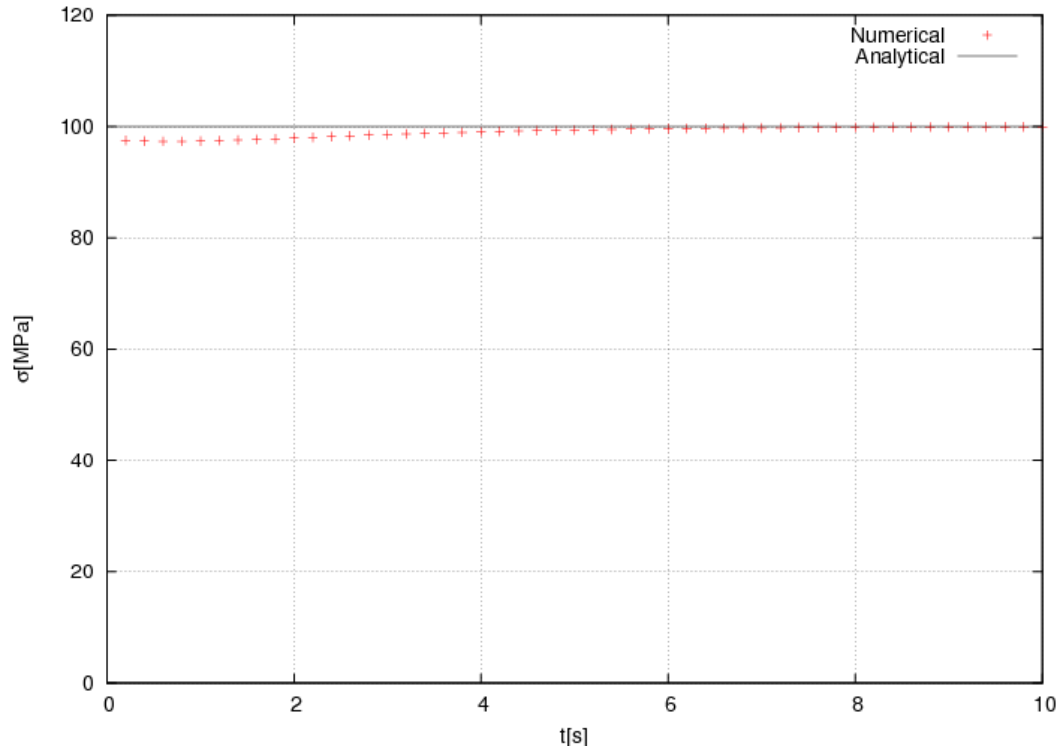

Figure 7: Stress history for creep test.

3.2 Constant strain-rate test

From the good results obtained previously for two basic tests in viscoelasticity it is possible to study other cases. In this subsection the viscoelastic problem for the particular case of constant strain-rate is addressed. This is another classic test for determining the mechanical behavior of time-dependent materials.

First, the simulations are carried out with the implementation for one point of Gauss where the sensitivity to constitutive parameters is studied. Next, the viscoelastic problem is studied with the finite element implementations.

3.2.1 Constant strain-rate test with different number of Maxwell-elements

The influence of number of branches in the generalized Maxwell model is studied in this case. The numerical simulations are performed with one Hooke-element and different number of Maxwell-elements, while the parameters μ_0, μ_j and τ_j are kept fixed. Thus, γ_j and η_j are the same in each branch of Maxwell.

The material properties are shown in Table 3. The strain changes linearly and has a value of $0< \varepsilon \leq 0.5$ with $\Delta\varepsilon=0.05$. The time interval considered is $0< t \leq 1$ with $\Delta t=0.1$.

$\mu_0=10$ N/mm^2
$\mu_j=10$ N/mm^2
$\eta_j=10$ MPa s ($\tau_j=1$s)

Table 3: Material properties.

The evolution of stress with strain for different number of Maxwell-elements is shown in Figure 8. As can be seen the stress response is nonlinear although the strain has a linear variation with time.

Furthermore, when the number of Maxwell-elements increases greater values of stress are obtained. This is highlighted in Figure 9, in which the influence of numbers of Maxwell-elements on the maximum stress σ_{max} reached it can be observed. The increase of Maxwell elements leads to greater values of σ_{max}.

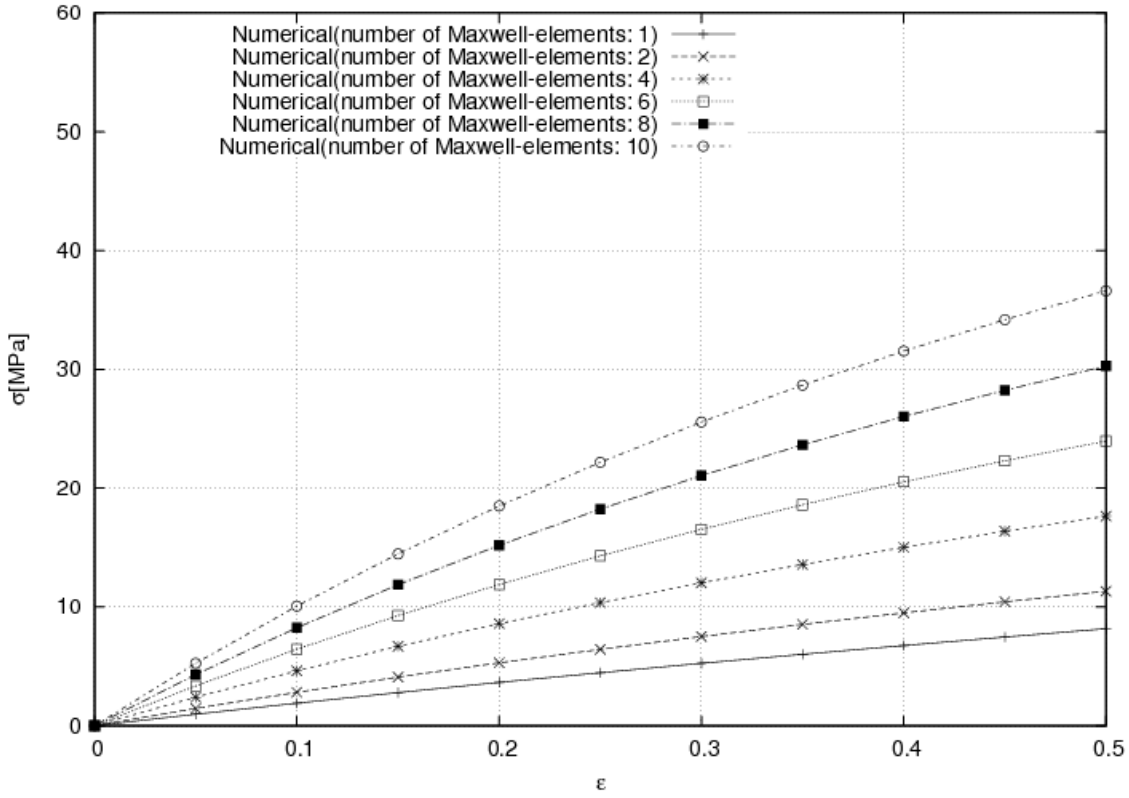

Figure 8: Stress versus strain for constant strain-rate. Different number of Maxwell-elements.

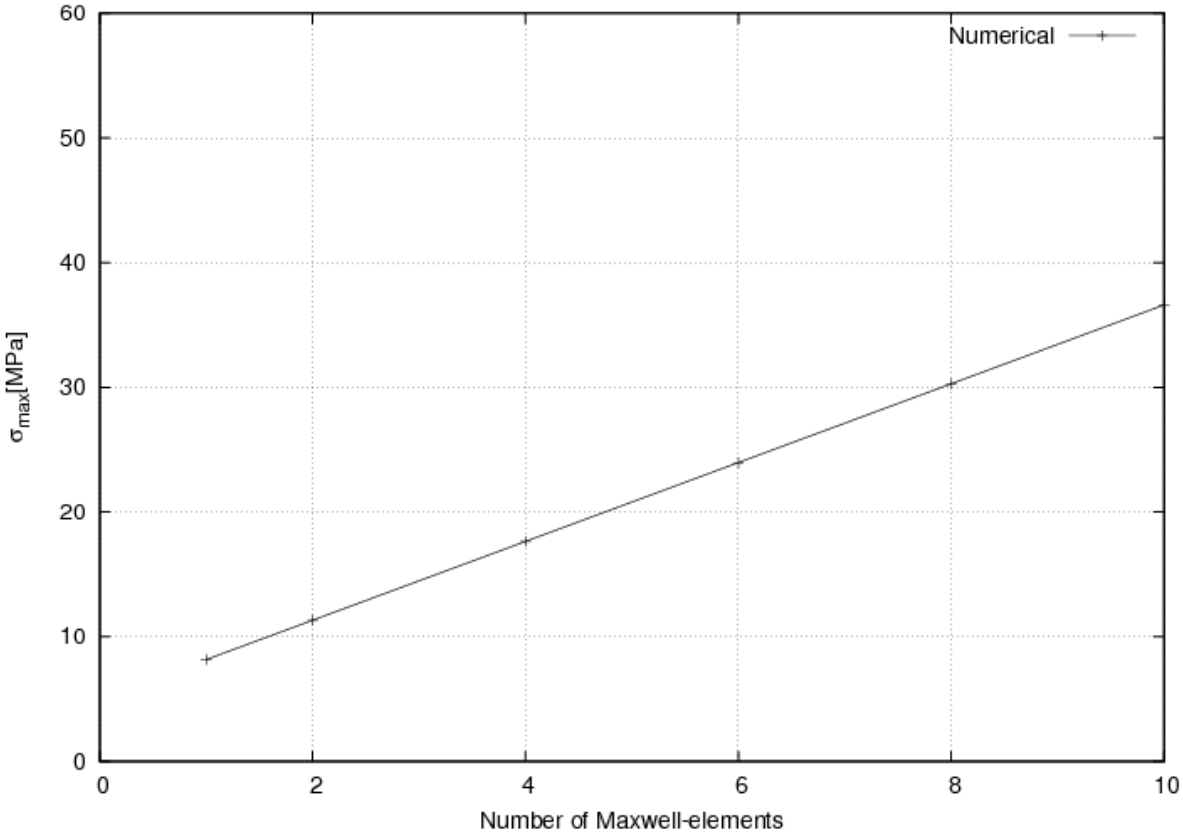

Figure 9: Sensitivity of σ_{max} to the number of Maxwell-elements.

3.2.2 Constant strain-rate test with different relaxation times

In this case the influence of different relaxation times on the generalized Maxwell model is studied with a fixed number of branches. The numerical simulations are carried out with ten Maxwell-elements and the same relaxation time in each branch. The material properties are shown in Table 4 with j=1..10. The applied strain and the time are the same as in 3.2.1.

μ_0=10 N/mm^2
μ_j=10 N/mm^2
η_j=1 MPa s (τ_j=0.1s)
η_j=5 MPa s (τ_j=0.5s)
η_j=10 MPa s (τ_j=1s)
η_j=50 MPa s (τ_j=5s)
η_j=100 MPa s (τ_j=10s)
η_j=200 MPa s (τ_j=20s)
η_j=200000 MPa s (τ_j=20000s)

Table 4: Material properties.

The stress-strain curves are shown in Figure 10. It can be seen that when τ_j increases (due to the viscosity η_j increases) greater values of stress are obtained. It should be noted that for values of τ_j higher to unity the responses are similar for different relaxation times and the values of stress are close to each other. Moreover, it should be noted that for τ_j equal to 20000 the stress strain relation is closed to the linear elastic limit case for η_j approaching to infinity. The linear elastic limit case corresponds to eleven elastic parallel springs. Since all the springs have equal elastic constant, the elastic equivalent constant is 110 N/mm^2 for the linear elastic limit case.

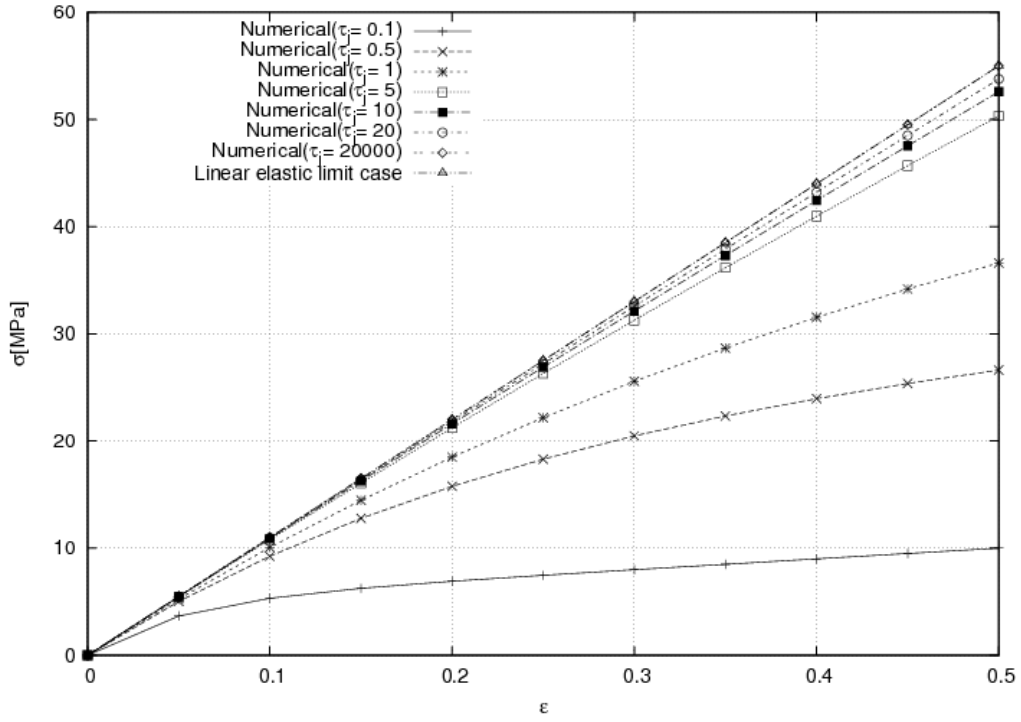

Figure 10: Stress versus strain for constant strain-rate. Different relaxation times.

Sensitivity of σ_{max} to the different relaxation times is plotted in Figure 11. It can be observed for values of τ_j equal or less than unity (τ_j =0.1,0.5,1) that σ_{max} is very sensitive to the change of relaxation time. Otherwise, for values of τ_j higher than unity (τ_j=5,10,20) the influence of this parameter on σ_{max} is small.

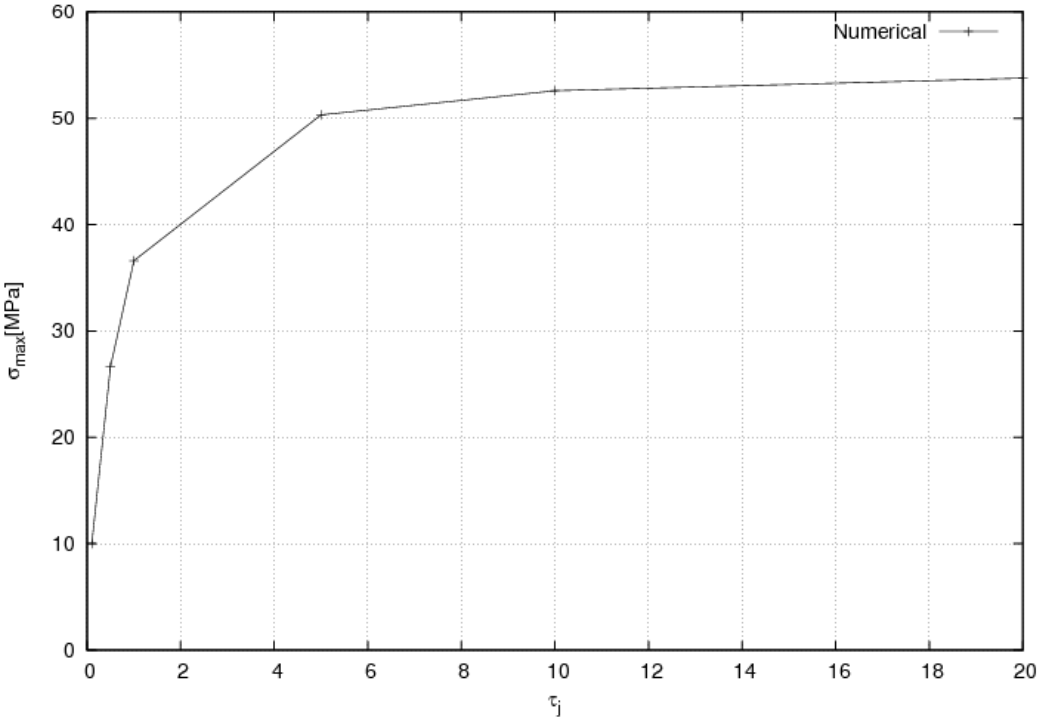

Figure 11: Sensitivity of σ_{max} to the different relaxation times.

3.2.3 Finite element simulations with one branch of Maxwell

Finally, the results from 3.2.1 are taken as references to validate the implementations and simulations carried out with 2D finite element code and Metafor. Here, the same properties as in 3.2.1 are considered together with a Poisson's ratio equal to 0.4995. The geometry and boundary conditions used in finite element codes are shown in Figure 12, where P is the applied load and is equal to 10N. In the simulations a plane strain problem with Q1 finite element type is considered.

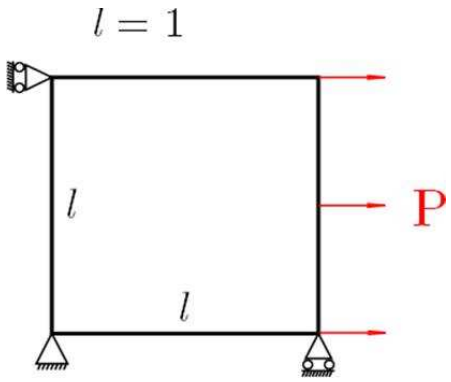

Figure 12: Geometry and boundary conditions.

The results obtained with the three numerical codes are plotted in Figure 13. The results from one point of Gauss/2D finite (linear) element implementations appear stiffer than Metafor. From a point of view of the global response it can be said that the three codes lead to similar results. It can be seen from Figure 13 that the difference reached for the stress (ε=0.05) is approximately equal to 12%.

It can be noted that the implementations in the finite element codes are only preliminary. Further studies are needed to validate these implementations.

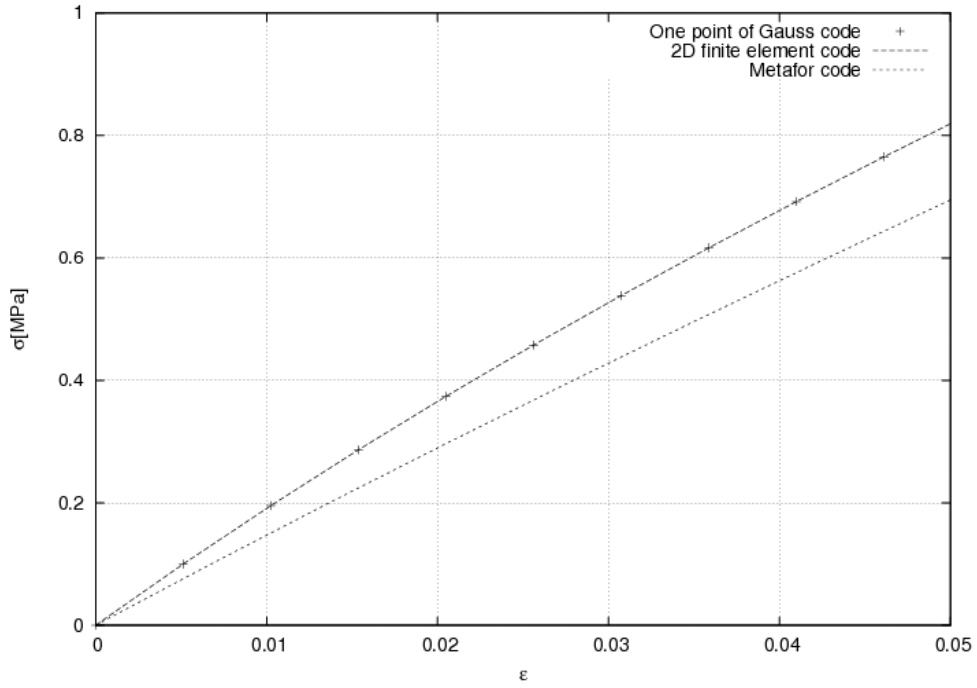

Figure 13: Stress versus strain.

4 CONCLUSIONS

In this work one point of Gauss code based on the numerical implementation addressed by Kaliske and Rothert (1997), able to reproduce the response of viscoelastic materials that can be modeled by a generalized Maxwell model have been developed. This code has been validated against classical tests used in viscoelasticity such as relaxation and creep, yielding very good results relative to analytical ones.

In addition, the generalized Maxwell model in two finite element codes has been implemented, with good results. Nevertheless, further work should focus on more detailed comparisons for the large strains finite element codes implementations.

Furthermore, the influence of constitutive parameters related to the viscoelastic behavior has been studied. For the case of constant strain-rate for different numbers of Maxwell-elements the increase of maximum stress occurs gradually. However, for the case of constant strain-rate with different relaxation times and a fixed number of branches the increase of maximum stress is not gradual, particularly for values of relaxation times equal or less than unity.

5 ACKNOWLEDGEMENTS

The financial support provided by project “A numerical framework for efficient time

integration of viscoelastic models submitted to large deformations. Applications to Biomechanical Engineering, BE/12/04, International Cooperation Area of MINCyT (Argentine) and FNRS (Belgium)" is gratefully acknowledged. The argentinean group acknowledges the support granted by SeCTyP-U.N.Cuyo projects

REFERENCES

Bekker, A., Kok, S., Cloete, T.J., and Nurick, G.N., Introducing objective power law rate dependence into a visco-elastic material model of bovine cortical bone. *International Journal of Impact Engineering*, 6:28-36, 2014.

Bonet J., Large strain viscoelastic constitutive models. *International Journal of Solids and Structures*, 38:2953-2968, 2001.

Careglio, C., García Garino, C., and Mirasso, A., SOGDE3D: Código de elastoplasticidad con grandes deformaciones 3D. *Mecánica Computacional*, XXIV: 363-373, 2005.

Drozdov, A.D., Finite elasticity and viscoelasticity: a course in the nonlinear mechanics of solids. World Scientific, 1996.

Fancello, E. A., Ponthot, J.-P., and Stainier, L., A variational formulation of constitutive model and updates in nonlinear finite viscoelasticity. *International Journal for Numerical Methods in Engineering*, 65:1831-1864, 2006.

Fancello, E. A., Ponthot, J.-P., and Stainier, L., A variational framework for nonlinear viscoelastic models in finite deformation regime. *Journal of Computational and Applied Mathematics*, 215:400-408, 2008.

García Garino, C., Un modelo numérico para el análisis de sólidos elastoplásticos sometidos a grandes deformaciones. PhD thesis, Universidad Politécnica de Catalunya, Barcelona, 1993.

García Garino, C., Gabaldón, F., and Goicolea, J.M., Finite element simulation of the simple tension test in metals. *Finite Elements in Analysis and Design*, 42:1187-1197, 2006.

Kaliske, M., and Rothert, H., Formulation and implementation of three-dimensional viscoelasticity at small and finite strains. C*omputational Mechanics*, 19: 228-239, 1997.

Lee, J.H., Finite element modeling of interfacial forces and contact stresses of pneumatic tire on fresh snow for combined longitudinal and lateral slips. *Journal of Terramechanics*, 48(3):171-197, 2011.

Ponthot, J.-P., Traitement unifié de la Mécanique des Milieux Continus solides en grandes transformations par la méthode des éléments finis. PhD thesis, Université de Liège, 1995.

Ponthot, J.-P., Unified stress update algorithm for the numerical simulation of large deformation elasto-plastic and elasto-viscoplastic processes. *International Journal of Plasticity*, 18:91–126, 2002.

Ottosen, N.S., and Ristinmaa, M., *The mechanics of constitutive modeling*. Elsevier, 2005.

Saidi, I., Gad, E.F., Wilson, J.L., and Haritos, N., Development of passive viscoelastic damper to attenuate excessive floor vibrations. *Engineering Structures*, 33: 3317-3328, 2011.

Shim, V.P.W., Yang, L.M., Liu, J.F., and Lee, V.S., Characterisation of the dynamic compressive mechanical properties of cancellous bone from the human cervical spine. *International Journal of Impact Engineering*, 32(1–4): 525-540, 2005.